Automation in Construction 111 (2020) 103050

Contents lists available at ScienceDirect

Automation in Construction

journal homepage: www.elsevier.com/locate/autcon

Risk assessment and management via multi-source information fusion for undersea tunnel construction

Hong Zhou[a,*], Yinghui Zhao[b], Qiang Shen[b], Liu Yang[c], Hubo Cai[d]

[a] Room 506, Zeng Chengkui Building, No.182, Daxue Road, Siming District, Xiamen 361005, Fujian, China
[b] Dept. of Civil Engineering, School of Architecture and Civil Engineering, Xiamen University, China
[c] Lyles School of Civil Engineering, Purdue University, United States of America
[d] Lyles School of Civil Engineering, Division of Construction Engineering and Management, Purdue University, United States of America

ARTICLE INFO

Keywords:
Undersea tunnel construction
Multi-source information fusion
Construction risk
D-S evidence theory
Fuzzy matter element

ABSTRACT

The construction of undersea tunnels is an extremely risky endeavor that is vulnerable to water seepage and gushing due to the high water pressure, complex geological conditions, and pore water trapped in unstable rocks. This risk can lead to the collapse of tunnels under construction and disastrous consequences of fatalities and injuries as well as project delays and financial losses. The current risk management practices for tunnel construction projects in China are static and rely on the subjective judgement of experts and practitioners and do not incorporate real-time monitoring data during the construction process at this time. This paper presents a new method and system to assess and manage the risks during the construction process by coupling the risk management system and the quality management system and integrating jobsite monitoring data, design data, and environmental data. In this new method and system, the risk factors are categorized into (hu)man, material, machine, method, and environment, or 4M1E, and are quantitatively measured. The Dempster-Shaffer (D-S) theory was adopted in this method to both fuse the 4M1E data and to compute the aggregate risk index. This new method and system was tested during the Xiamen Metro Line No. 3 project when a shield machine cutter accident occurred. The results show that, before the accident, the individual risk measures in all five dimensions (4M1E) and the aggregate risk index were extremely high, which clearly illustrated the feasibility and capability of the newly developed method and system.

1. Introduction

Undersea tunneling, an essential component in many metro line infrastructure projects in coastal areas, is an extremely risky endeavor. As the shield machine drills through the underground space, the high water pressure, complex geological conditions, and pore water trapped in unstable rocks can cause water seepage and gushing that can result in devastating accidents on a large scale. For example, in China, a total of 246 tunneling accidents were reported between 2012 and March 2016 with an average of 1.44 accidents per week. An accident that occurred on February 12, 2017 during the tunneling process of an undersea section of Xiamen Metro Line No. 2 led to three unfortunate deaths as well as project delays and financial losses. Also, a shield cutter accident on the Xiamen Metro Line No. 3 caused a six-month delay and led to a financial loss of nearly 20 million RMB (2.98 million US dollars). Considering that the total infrastructure investment in subway projects in China reached nearly 4080 billion RMB (583 billion US dollars) involving at least 18 metro lines involved undersea tunneling in the most recent ten years, risk management in undersea tunneling has become a top national priority.

The current practices in risk assessment and management have three limitations that have become the major barriers to their adoption in managing the risks in undersea tunneling projects. First, risk assessment typically relies on surveys and expert opinions, which is subjective in both the identified risks and their quantification [1–3]. Second, risk assessment is typically performed before construction commences and is a static, one-time effort with no capacity to incorporate real-time monitoring data or to update the risks as construction progresses. Third, the existing risk indexing systems are not unified, which makes it difficult to apply the findings and lessons learned from one project to another [4–9]. A critical need therefore exists to develop a method for incorporating construction monitoring

* Corresponding author at: School of Architecture and Civil Engineering, Xiamen Engineering Technology Center for Intelligent Maintenance of Infrastructures, Xiamen University, China.
E-mail address: mcwangzh@xmu.edu.cn (H. Zhou).

https://doi.org/10.1016/j.autcon.2019.103050
Received 26 May 2019; Received in revised form 11 November 2019; Accepted 6 December 2019
Available online 03 January 2020
0926-5805/

data and then to be able to assess the risks dynamically and quantitatively in a unified format as the project progresses.

This paper introduces a new method and system to dynamically assess and manage risks in undersea tunneling projects during the construction process by coupling a project's quality management system and risk management system and integrating jobsite data, design data, and environmental data via multi-source information fusion. The rationale for this new method and system is that quality and risk are two sides of the same coin: 1) quality is the measure of meeting requirements and 2) risk is the deviation from the requirements under adverse conditions [10]. Therefore, the risk and quality management systems are intertwined and feature recognition of quality can be used to identify and quantitatively assess the risks. In the new method and system, the risk factors are categorized into (hu)man, material, machine, method, and environment, or 4M1E. The Dempster-Shaffer (D-S) evidence theory was adopted to fuse the 4M1E data to compute the uniform aggregate risk indices. Data management and risk visualization are realized through a building information modeling (BIM) platform that facilitates communications and holistic risk management. The new method and system was tested during the Metro Line No. 3 project in Xiamen, China. Our results confirmed that this system is able to detect and assess risks as a project progresses to provide early warnings and prevent accidents during the undersea tunneling process.

2. Background and reviews of related studies

This section provides background information on shield tunneling construction and reviews the related studies in the areas of integrated quality and risk management, quantitative assessment of risks, data fusion through D-S theory, and the use of BIM in data management and visualization.

2.1. Tunneling construction using shield machine

Modern tunneling construction typically uses a tunnel boring machine (TBM), which is a shield machine that can achieve a high-level of mechanized construction to improve productivity and enhance safety. A shield machine is not affected by landform and weather conditions and can reach a drilling speed of 600 m per month in medium and hard rock stratum with little influence from the seabed geological structure. The two main types of shield machines are the Earth Pressure Balance (EPB) and the Slurry Shield (SS). Fig. 1 illustrates these two types with EPB on the left and SS on the right. The EPB shield is generally used in places where there is a medium water content and a weak consolidation of sandy soil stratum. The SS type is more often adopted in places where there is a high-water content and a high or weak consolidation stratum. Despite the advantages of tunneling machines as far as safety and productivity, accidents such as collapse, water gushing, and sand gushing still occur in tunneling projects where a tunnel boring machine is used, which are later attributed to the (hu)man, materials, and machine risks [11].

2.2. Quantitative risk assessment based on quality factors

Construction risks are uncertain, and it is therefore very difficult to determine probability distribution functions for construction risks. The most commonly used method for risk identification and assessment utilizes expert opinions and judgments, which is often subjective and qualitative [4–8,14,15].

On the other hand, most quality factors are quantitative and measurable. From the risk perspective, quality can be viewed as the risk of failing to meet the needs and expectations of stakeholders and achieving their values; and potential failure sources can be identified, processed, and eliminated by using measurements of quality control variables [16]. Risk and quality are two interrelated tasks with a strong correlation in project management [17,18]; and quality management and risk management are complementary to each other and can be integrated [10,19]. Considering the complementary relationship between quality management and risk management, a potential solution for quantitatively assessing risk is to use quantitative quality measures to discover the uncertainty.

Along this line of thought, Maria [10] suggested that the integration of quality management and risk management greatly simplifies the number of structures, processes, resources, and files in an organization and improves the performance of a holistic management system with a synergistic effect. The concept of an “integrated management system (IMS)” was proposed correspondingly [20]. The integration of a quality management system (QMS) and a risk management system (RMS) effectively reduces resource waste and contributes to the synergy of the technology, program, organization, and cultural environment. Katarina [21] concluded that an IMS that integrates quality management (ISO9001), environmental management (ISO14000), and health management (OHSAS18001) can significantly improve the management efficiency of construction companies and further suggested integrating additional management systems (such as risk management) to take full advantage of an IMS.

In the practice of quality management, the factors that are used to measure the quality levels can be classified into five categories: (hu)man, material, machine, method, and environment, which are referred to as 4M1E. This classification of quality factors is a widely accepted framework in quality management [22–24]. Consequently, the risk factors in construction also can be classified as 4M1E and identified and assessed correspondingly. For example, using the environment factor, the environmental risk can be assessed through the quality of the rock.

A few studies attempted to adopt the 4M1E framework in risk assessment and management. Yuan [4] described the risk-causing mechanism as follows. “A man may have work accidents, materials may have defects, machines may fail, inappropriate method seriously affects quality, and environment may cause natural disasters.” Fig. 2 provides a graphical illustration of the mechanism which connects the risk factors, risk environment, risks, and risk losses. Liu [5] developed a risk index system considering the 4M1E risks and constructed a comprehensive risk assessment model using a rough set and a neural network. Wu [6] incorporated 4M1E as an external factor to evaluate the safety

Fig. 1. EPB (left) and SS (right) [12,13].

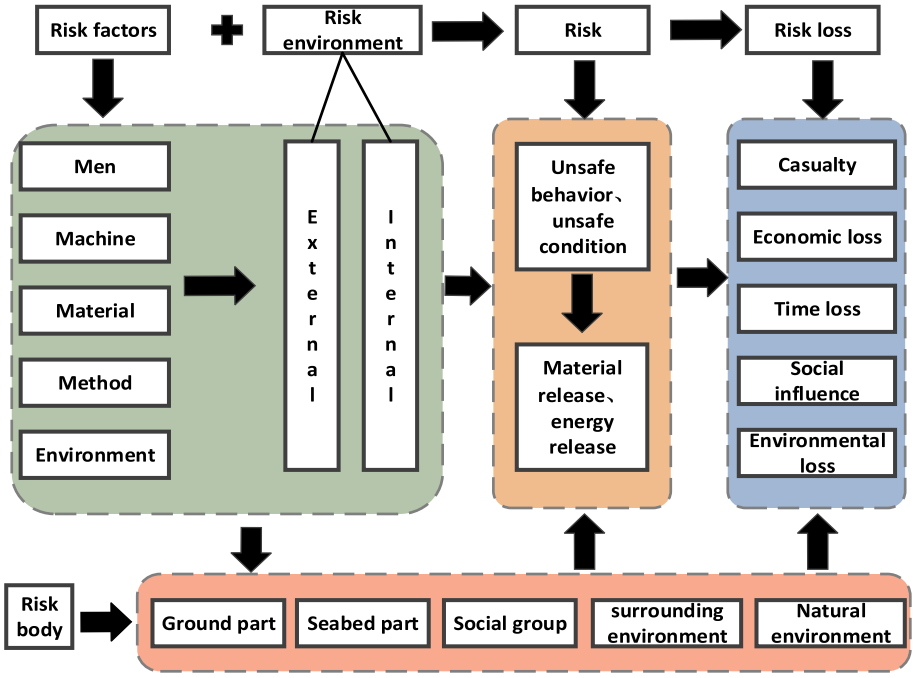

Fig. 2. Mechanism of construction risk based on 4M1E.

damage to a road surface during shield tunneling. Haize [7] built a risk assessment system for subway shield tunnel seepage based on 4M1E. Liu [8] developed a questionnaire on the safety risk factors of subway construction by combining exploratory factor analysis (EFA) and a structural equation model (SEM), which showed that construction risk factors can be grouped into 4M1E.

However, it is inappropriate to directly copy the 4M1E framework from quality management to risk management and use the quality factors directly for two main reasons. First, direct mapping between risk factors and quality factors does not exist and second, no unified risk evaluation index system exists. These two knowledge gaps are addressed by this new method and system, which establishes a connection between quality measures and risk factors and developing a corresponding unified risk index system.

2.3. BIM for integrated quality and risk management

Building information modeling (BIM) has emerged as a powerful platform to integrate quality inspection results into the product model for quality management. It has been widely used in construction quality management and has great potential for serving as an advanced platform to integrate quality and risk and improve the efficiency of quality management and risk management at the same time.

In the field of construction risk management, Ding et al. [25,26] established a BIM-based risk identification expert system for subway construction management that integrated BIM, information extraction, knowledge-based management, and risk identification. Du [27] developed an early warning and risk management system to dynamically monitor large and high-risk construction equipment and manage the risk to surrounding buildings during the subway construction process by combining a geographical information system (GIS), a global positioning system (GPS), and a BIM.

In the field of construction quality management, Ding et al. [28] integrated construction quality, which included product, organization, and process information, into a BIM and extended the 3D BIM to n-D BIM to achieve real-time quality management on the jobsite. Wang [29] established a construction quality control system by integrating a BIM and light detection and ranging (LiDAR) for real-time collection and processing of field quality information. Wang's system also can effectively identify potential construction defects, support real-time quality control, and overcome the drawbacks (e.g., time-consuming and inefficient) in current construction quality control practices.

Despite its successes, BIM still lacks the ability to assess construction activities, use sensor data, and evoke control algorithms in real time to provide timely solutions to minimize risk while ensuring quality during construction. A few studies attempted to find a solution to this problem. Chen [30] developed a computer-based risk assessment system for standardized quality control and quality defect reduction. However, Chen's model is static and does not perform well when handling dynamic risk problems, which happens often in the construction industry. Srinivasan [31] proposed a preliminary Dynamic-BIM (D-BIM) approach for continuous monitoring of construction performance through a timely feedback system, which has great potential for applying BIM in dynamic problems.

Motivated by BIM's potential in the area of integrated quality and risk management, we designed a central BIM platform for the implementation and visualization of risk management in undersea tunneling projects. Fig. 3 illustrates the overall structure of the platform, where the quality measures and risk indices are dynamically updated as the project progresses and synchronized with the BIM model.

2.4. Dempster-Shaffer (D-S) evidence theory

Synthesizing multi-source information always has been a challenge, especially in construction risk management where a variety of heterogeneous data from multiple sources is involved. Relevant data exist in many forms, such as textual documents, photos, videos, 3-D models, and GIS data (for the geospatial surroundings). Adding to the complexity of the challenge, these data may be incomplete, inaccurate, and uncertain and also may contain noise. How to synthesize multi-source information that has different levels of uncertainty, fuzziness, contradictions, and errors is a challenging task in complex multi-objective decision problems. Data fusion has emerged as a promising approach to combining multi-source data of heterogeneous formats and quality to obtain accurate estimates of the target information. For example, Pradhan [32] introduced such a method into construction productivity analysis, and Pradhan et al. [33] formalized dynamic queries to support data fusion for monitoring construction productivity. Razavi and Haas

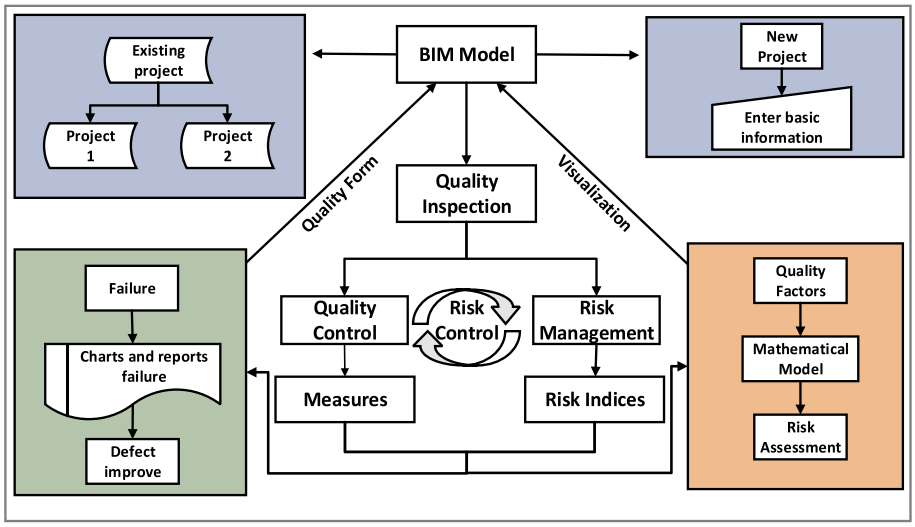

Fig. 3. A BIM platform for integrated quality and risk management.

[34] developed a method to fuse multisensory data to track materials on construction jobsites. Shahandashti summarized some application examples of data fusion in civil engineering and pointed out a few advantages of data fusion in civil engineering applications [35].

Among the many methods for information and data fusion, D-S evidence theory has an adaptive and flexible algorithm that enables reasoning with uncertainty and fusing heterogeneous data that are full of randomness, fuzziness, and uncertainties from multiple sources [36]. D-S evidence theory has the capacity to deal with uncertain information based on the "evidence body" and "fusion" [37]. It has been widely used in fields such as expert systems where decisions must be made based on data that might not be complete and accurate [35]. Construction risk management relies on data that requires uncertainty modeling and information integration in the context of multi-objective decision-making. This characteristic motivated the adoption of the D-S evidence theory in the new method and system proposed in this paper.

3. Precise risk assessment and management based on 4M1E multi-source information fusion

The new precise risk assessment and management method and system presented in this paper was developed specifically to manage construction risks in undersea tunneling projects. Fig. 4 illustrates the overall framework based on the fusion of 4M1E data. The framework is composed of three modules: 1) the 4M1E-work breakdown structure (WBS) module, 2) the risk assessment module, and 3) the BIM module for risk visualization and management. The integration of BIM, D-S evidence theory, and fuzzy matter element (FME) enables the fusion of data from multiple sources to precisely assess the risk in tunneling projects.

3.1. 4M1E-WBS module

The 4M1E-WBS module breaks down the construction tasks into multiple interconnected sub-units that are aligned with a project's progress. This decomposition enables the risk and quality assessment at the individual sub-unit level by considering the five categories of 4M1E. Since these sub-units are interconnected and aligned with the project's progress, the resulting risk control is dynamic in that both risk assessment and management are updated as the project progresses and the status of the sub-units proceeds from planned to ongoing and completed.

3.2. Risk assessment module

The risk assessment module fuses the multi-source 4M1E quality factors to assess the risks and thereby avoids the subjective bias in expert scoring and judgement. This module is the core module of the newly developed method and system. Its two main compartments are the risk index system and the data fusion algorithm based on the D-S evidence theory.

3.2.1. 4M1E risk index system for undersea shield tunneling

The new 4M1E risk index system is composed of the individual risk factors (grouped under the five categories of 4M1E), the risk indices for each category, and the overall risk index. A risk factor is assessed using one or more measures. To identify the risk factors in this study, the data of 123 subway accidents in 23 cities in China between 2001 and 2018 were acquired and processed through the R language [38]. This effort resulted in 16 risk factors and 43 measures in the categories of machine, material, method, and environment. In addition, three risk factors based on the role of field crew (i.e., worker, technician, and manager) and five measures were identified for the (hu)man category. Fig. 5 illustrates the individual risk factors and their corresponding categories. This structure allows the hierarchical computation of risks at the individual risk factor level, the main category level, and the overall level for specific WBS sub-units.

Due to the complexities of various tunneling environments, the interval identification of various influencing factors can be vague. The reasonable interval division of each factor is carried out by combining engineering practice and a large amount of accumulated expert experience [39]. The measures for individual risk factors are further classified into five ranges from I to V, and the index classification is mainly based on the even distribution according to Zhang (2017) [36] and Wu (2018) [40] in security risk perception. The specific numeric range of each index grade is divided according to the construction site specification. Table 1 lists the risk factor measures that do not follow the even distribution and the references that were consulted to develop the specific classifications. Risk factors are interactive, and their assessment must consider the influence from each other. For example, the geological environment affects the blade speed (i.e., a suitable geological environment allows higher speeds than a poor geological environment). As such, in setting the range for the blade speed measure of the driving parameters of the shield machine risk factor, the difference between the actual speed and the control speed, which is determined based on the geological environment and site conditions rather than the actual speed, is used to incorporate the cross-category influences of the

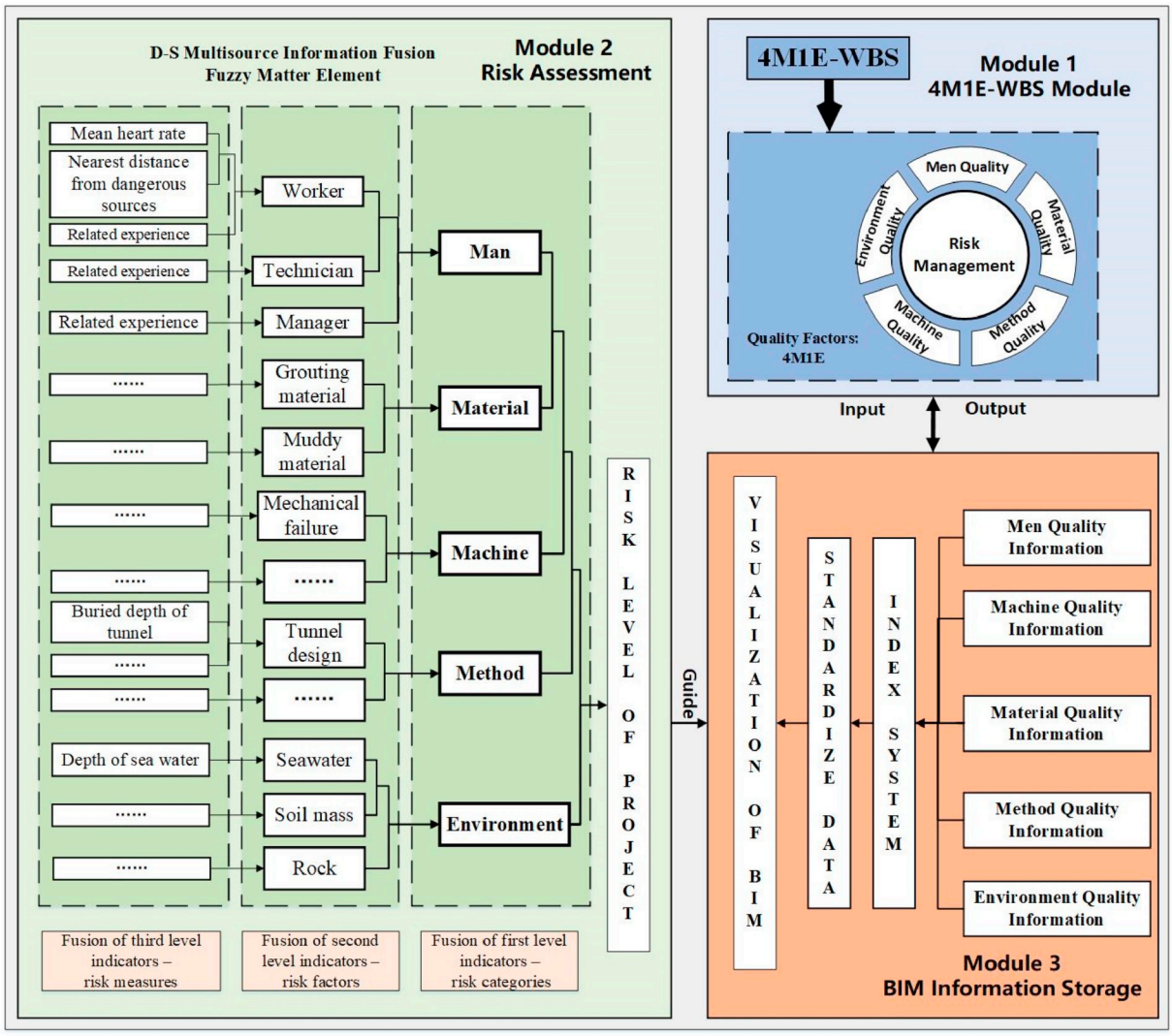

Fig. 4. Construction risk management based on 4M1E and multi-source information fusion.

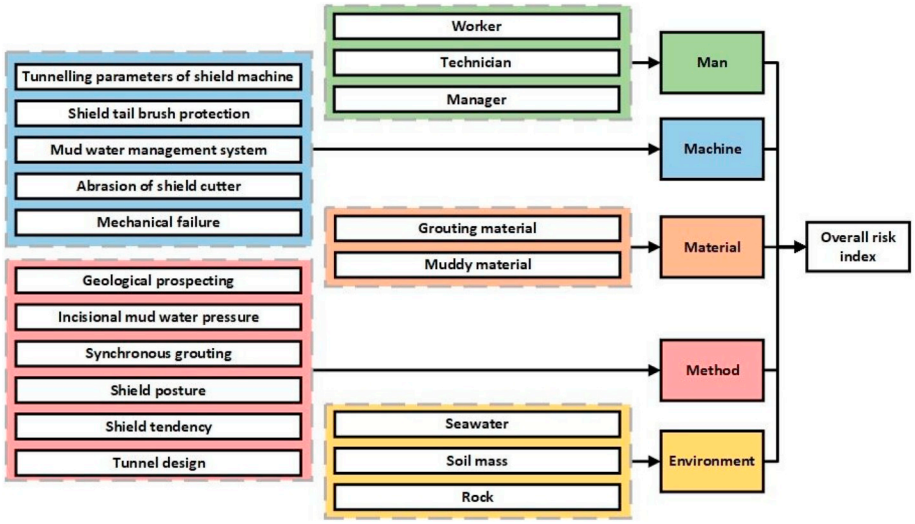

Fig. 5. Construction risk index system of subsea tunnel.

Table 1
Risk factor measures that do not follow the even distribution.

Indicator	Basis of classification
Mean heart rate	The relationship between heart rate and fatigue [41–43]
Related experience (for Worker) Related experience (for Technician) Related experience (for Manager)	Construction hazard identification and risk assessment [44–46]
Oil injection volume (deviation from control value)	The effect of oil injection volume control on leakage slurry in shield tail [47,48]
7 days compressive strength	The performance requirements for subsea tunnel grouting material [49]

risk factors. The measures that take into account the control values are indicated in Table 2. Also, Table 2 lists the classifications of all the measures for the individual risk factors, grouped in the five categories of 4M1E.

The indices of multi-source data need to be normalized to become dimensionless and comparable. Table 3 illustrates the normalization results of risk measures. Depending on whether the impact on the risk is positive or negative, the normalization computation is different. If an index factor has a negative impact on the tunneling risk, then the greater its value is and the less the risk there will be. As such, normalization follows Eq. (1).

$$c_i' = (c_{i\max} - c_i)/(c_{i\max} - c_{i\min}) \quad (1)$$

where c_i' is the normalized index factor, c_i is the measured value and $c_{i\max}$ and $c_{i\min}$ are the maximum and minimum value of the index

Table 2
Risk index classification of sub-sea tunnel shield construction method.

Indicator				I	II	III	IV	V
(hu)Man factors	C_1	Worker	Mean heart rate	0–81	81–98	98–116	116–128	128–150
	C_2		Nearest distance from dangerous sources	1.6–2	1.2–1.6	0.8–1.2	0.4–0.8	0–0.4
	C_3		Related experience	15–20	10–15	5–10	3–5	0–3
	C_4	Technician	Related experience	15–20	10–15	5–10	3–5	0–3
	C_5	Manager	Related experience	15–20	10–15	5–10	3–5	0–3
Machine factors	C_6	Driving parameters of shield	Driving speed of shield machine	0–10	10–20	20–30	30–40	40–50
	C_7	machine	Total thrust of lifting jack (deviation from experience value)	0–1000	1000–2000	2000–3000	3000–4000	4000–5000
	C_8		Penetration of cutter disc	0–5	5–10	10–15	15–20	20–25
	C_9		Blade speed (deviation from control value)	0–0.1	0.1–0.2	0.2–0.3	0.3–0.4	0.4–0.5
	C_{10}		Cutter disc torque (deviation from experience value)	0–100	100–200	200–300	300–400	400–500
	C_{11}	Shield tail brush protection	Oil injection volume (deviation from control value)	0	0–5	5–10	10–15	15–50
	C_{12}		Shield machine tail gap (deviation from control value)	0–5	5–10	10–15	15–20	20–25
	C_{13}	Mud water integrated Management system	Pressure variation in upper mud water storehouse	0–0.1	0.1–0.2	0.2–0.3	0.3–0.4	0.4–0.5
	C_{14}		Pressure variation in medium mud water storehouse	0–0.1	0.1–0.2	0.2–0.3	0.3–0.4	0.4–0.5
	C_{15}		Air pressure change range of air cushion bin	0–0.1	0.1–0.2	0.2–0.3	0.3–0.4	0.4–0.5
	C_{16}	Cutter disc wear	Edge hob wear	0–3	3–6	6–9	9–12	12–15
	C_{17}		Roll tool ring wear	0–5	5–10	10–15	15–20	20–25
	C_{18}		Center hob wear	0–5	5–10	10–15	15–20	20–25
	C_{19}	Mechanical failure	Early warning system failure	0–0.2	0.2–0.4	0.4–0.6	0.6–0.8	0.8–1
Material factors	C_{20}	Grouting material	7 days Compressive strength	2–3	1–2	0.5–1	0.15–0.5	0–0.15
	C_{21}		28 days compressive strength	4–5	3–4	2–3	1–2	0–1
	C_{22}	Muddy material	Mud weight (deviation from control value)	0	0–0.05	0.05–0.1	0.1–0.15	0.15–0.2
	C_{23}		Viscosity of mud water (deviation from control value)	0	0–1	0–1	2–3	3–4
Method factors	C_{24}	Geological prospective	Pitch of holes	0–2	2–4	4–6	6–8	8–10
	C_{25}	Incisional water pressure	Deviation from set value	0–0.02	0.02–0.04	0.04–0.06	0.06–0.08	0.08–0.10
	C_{26}	Synchro grouting	Grouting volume (deviation from control value)	0	0–0.5	0.5–1	1–1.5	1.5–2
	C_{27}		Grouting pressure (deviation from control value)	0	0–0.1	0.1–0.2	0.2–0.3	0.3–0.4
	C_{28}	Shield posture	Plane deviation of incision	0–20	20–40	40–60	60–80	80–100
	C_{29}		Height deviation of incision	0–20	20–40	40–60	60–80	80–100
	C_{30}		Shield tail plane deviation	0–20	20–40	40–60	60–80	80–100
	C_{31}		Shield tail elevation deviation	0–20	20–40	40–60	60–80	80–100
	C_{32}	Shield trend	Horizontal trend	0–1	1–2	2–4	4–6	6–8
	C_{33}		Vertical trend	0–1	1–2	2–4	4–6	6–8
	C_{34}	Tunnel design	Buried depth of tunnel	28–40	18–28	12–18	6–12	0–6
	C_{35}		Tunnel thickness span ratio	3–5	2–3	1–2	0.5–1	0–0.5
	C_{36}		Tunnel span	0–7	7–10	10–12	12–15	15–25
	C_{37}		Tunnel height span ratio	0.7–1	0.65–0.7	0.6–0.65	0.5–0.6	0–0.5
Environment factors	C_{38}	Sea	Depth of sea water	0–5	5–10	10–15	15–20	20–25
	C_{39}	Soil	Natural water content	0–20	20–40	40–60	60–80	80–100
	C_{40}		Natural void ratio	0.6–0.7	0.7–0.8	0.8–0.9	0.9–1.0	1.0–1.1
	C_{41}		Liquid limit	75–100	60–75	45–60	30–45	0–30
	C_{42}		Liquidity index	−0.5–0	0–0.25	0.25–0.75	0.75–1	1–1.5
	C_{43}		Compression modulus	30–50	20–30	10–20	5–10	0–5
	C_{44}		Poisson ratio	0.4–0.5	0.3–0.4	0.2–0.3	0.1–0.2	0–0.1
	C_{45}	Rock	Rock integrity index	0.75–1	0.55–0.75	0.35–0.55	0.15–0.35	0–0.15
	C_{46}		Uniaxial compressive strength	250–300	100–250	50–100	25–50	0–25
	C_{47}		Rock quality designation	90–100	75–90	50–75	25–50	0–25
	C_{48}		Permeability coefficient	0–1	1–3	3–5	5–10	10–20

Table 3
Classification of dimensionless risk indicators.

Indicator				I	II	III	IV	V
(hu)Man factors	C_1	Worker	Mean heart rate	0–0.540	0.540–0.653	0.653–0.773	0.773–0.853	0.853–1
	C_2		Nearest distance from dangerous sources	0–0.2	0.2–0.4	0.4–0.6	0.6–0.8	0.8–1
	C_3		Related experience	0–0.25	0.25–0.5	0.5–0.75	0.75–0.85	0.85–1
	C_4	Technician	Related experience	0–0.25	0.25–0.5	0.5–0.75	0.75–0.85	0.85–1
	C_5	Manager	Related experience	0–0.25	0.25–0.5	0.5–0.75	0.75–0.85	0.85–1
Machine factors	C_6	Driving parameters of shield	Driving speed of shield machine	0–0.2	0.2–0.4	0.4–0.6	0.6–0.8	0.8–1
	C_7	machine	Total thrust of lifting jack (deviation from experience value)	0–0.2	0.2–0.4	0.4–0.6	0.6–0.8	0.8–1
	C_8		Penetration of cutter disc	0–0.2	0.2–0.4	0.4–0.6	0.6–0.8	0.8–1
	C_9		Blade speed (deviation from control value)	0–0.2	0.2–0.4	0.4–0.6	0.6–0.8	0.8–1
	C_{10}		Cutter disc torque (deviation from experience value)	0–0.2	0.2–0.4	0.4–0.6	0.6–0.8	0.8–1
	C_{11}	Shield tail brush protection	Oil injection volume (deviation from control value)	0	0–0.1	0.1–0.2	0.2–0.3	0.3–1
	C_{12}		Shield machine tail gap (and control value deviation)	0–0.2	0.2–0.4	0.4–0.6	0.6–0.8	0.8–1
	C_{13}	Mud water integrated management system	Pressure variation in upper mud water storehouse	0–0.2	0.2–0.4	0.4–0.6	0.6–0.8	0.8–1
	C_{14}		Pressure variation in medium mud water storehouse	0–0.2	0.2–0.4	0.4–0.6	0.6–0.8	0.8–1
	C_{15}		Air pressure change range of air cushion bin	0–0.2	0.2–0.4	0.4–0.6	0.6–0.8	0.8–1
	C_{16}	Cutter disc wear	Edge hob wear	0–0.2	0.2–0.4	0.4–0.6	0.6–0.8	0.8–1
	C_{17}		Roll tool ring wear	0–0.2	0.2–0.4	0.4–0.6	0.6–0.8	0.8–1
	C_{18}		Center hob wear	0–0.2	0.2–0.4	0.4–0.6	0.6–0.8	0.8–1
	C_{19}	Mechanical failure	Early warning system failure	0–0.2	0.2–0.4	0.4–0.6	0.6–0.8	0.8–1
Material factors	C_{20}	Grouting material	7 days Compressive strength	0–0.333	0.333–0.666	0.666–0.833	0.833–0.95	0.95–1
	C_{21}		28 days compressive strength	0–0.2	0.2–0.4	0.4–0.6	0.6–0.8	0.8–1
	C_{22}	Muddy material	Mud weight (deviation from control value)	0	0–0.25	0.25–0.5	0.5–0.75	0.75–1
	C_{23}		Viscosity of mud water (deviation from control value)	0	0–0.25	0.25–0.5	0.5–0.75	0.75–1
Method factors	C_{24}	Geological prospective	Pitch of holes	0–0.2	0.2–0.4	0.4–0.6	0.6–0.8	0.8–1
	C_{25}	Incisional water pressure	Deviation from set value	0–0.2	0.2–0.4	0.4–0.6	0.6–0.8	0.8–0.10
	C_{26}	Synchro grouting	Grouting volume (deviation from control value)	0	0–0.25	0.25–0.5	0.5–0.75	0.75–1
	C_{27}		Grouting pressure (deviation from control value)	0	0–0.25	0.25–0.5	0.5–0.75	0.75–1
	C_{28}	Shield posture	Plane deviation of incision	0–0.2	0.2–0.4	0.4–0.6	0.6–0.8	0.8–1
	C_{29}		Height deviation of incision	0–0.2	0.2–0.4	0.4–0.6	0.6–0.8	0.8–1
	C_{30}		Shield tail plane deviation	0–0.2	0.2–0.4	0.4–0.6	0.6–0.8	0.8–1
	C_{31}		Shield tail elevation deviation	0–0.2	0.2–0.4	0.4–0.6	0.6–0.8	0.8–1
	C_{32}	Shield trend	Horizontal trend	0–0.125	0.125–0.25	0.25–0.5	0.5–0.75	0.75–1
	C_{33}		Vertical trend	0–0.125	0.125–0.25	0.25–0.5	0.5–0.75	0.75–1
	C_{34}	Tunnel design	Buried depth of tunnel	0–0.3	0.3–0.55	0.55–0.7	0.7–0.85	0.85–1
	C_{35}		Tunnel thickness span ratio	0–0.4	0.4–0.6	0.6–0.8	0.8–0.9	0.9–1
	C_{36}		Tunnel span	0–0.28	0.28–0.4	0.4–0.48	0.48–0.6	0.6–1
	C_{37}		Tunnel height span ratio	0–0.3	0.3–0.35	0.35–0.4	0.4–0.5	0.5–1
Environment factors	C_{38}	Sea	Depth of sea water	0–0.2	0.2–0.4	0.4–0.6	0.6–0.8	0.8–1
	C_{39}	Soil	Natural water content	0–0.2	0.2–0.4	0.4–0.6	0.6–0.8	0.8–1
	C_{40}		Natural void ratio	0–0.2	0.2–0.4	0.4–0.6	0.6–0.8	0.8–1
	C_{41}		Liquid limit	0–0.25	0.25–0.4	0.4–0.55	0.55–0.7	0.7–1
	C_{42}		Liquidity index	0–0.25	0.25–0.375	0.375–0.625	0.625–0.75	0.75–1
	C_{43}		Compression modulus	0–0.4	0.4–0.6	0.6–0.8	0.8–0.9	0.9–1
	C_{44}		Poisson ratio	0–0.4	0.4–0.6	0.6–0.8	0.8–0.9	0.9–1
	C_{45}	Rock	Rock integrity index	0–0.25	0.25–0.45	0.45–0.65	0.65–0.85	0.85–1
	C_{46}		Uniaxial compressive strength	0–0.167	0.167–0.667	0.667–0.833	0.833–0.917	0.917–1
	C_{47}		Rock quality designation	0–0.1	0.1–0.25	0.25–0.5	0.5–0.75	0.75–1
	C_{48}		Permeability coefficient	0–0.05	0.05–0.15	0.15–0.25	0.25–0.5	0.5–1

factor, respectively.

On the other hand, if the index factor has a positive impact on the tunneling risk, then the greater the value is and the more likely the risk will be. Eq. (2) illustrates the normalization process for this type of risk factors.

$$c_i' = (c_i - c_{i\min})/(c_{i\max} - c_{i\min}) \quad (2)$$

Taking the shield machine as an example, the daily driving distance (C_6) has a positive effect on the tunneling risk, and its normalization follows Eq. (2). For a value of 3.4 m, it is normalized to be 0.068 (calculated as follows), which belongs to Class I.

$$c_6' = \frac{c_6 - c_{6\min}}{c_{6\max} - c_{6\min}} = \frac{3.4 - 0}{50 - 0} = 0.068$$

In another case, the nearest distance from dangerous sources (C_2) has a negative effect, so for a value of 0.6 m, it is normalized to be 0.7 (calculated as follows), which belongs to Class I. Note in both cases, the classification remains the same.

$$c_2' = \frac{c_{2\max} - c_2}{c_{2\max} - c_{2\min}} = \frac{2 - 0.6}{2 - 0} = 0.7$$

3.2.2. Information fusion via D-S evidence theory

Although D-S evidence theory is widely accepted for fusing heterogeneous data, it has three limitations that must be addressed.

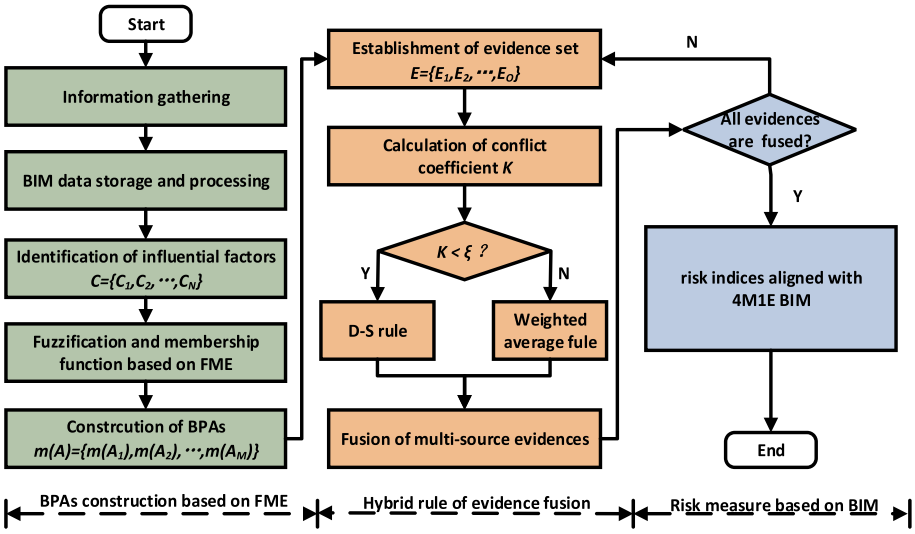

Fig. 6. FME and evidence fusion construction risks.

1) Traditional Dempster rules are incapable of handling highly conflicting evidence and can lead to unexpected and counter-intuitive results [50].

2) Effective applications of D-S evidence theory depends largely on generating BPAs, which is essentially a distribution modeling problem surrounding a random set of variables. The construction of BPAs is often closely related to their application. Since BPAs determine the fuzziness and randomness of the process, constructing them is a crucial problem [51].

3) Due to measurement errors and (hu)man factors, there may be unavoidable deviations or errors in observed data or evidence from multiple sources [52].

To address these limitations, this paper proposes a new method and system that incorporates an improved multivariate data fusion method and integrates D-S evidence theory, FME, and BIM. Implementation of the D-S evidence theory algorithm involves two steps: 1) establishment of the BPAs for the multi-source evidence body based on FME and 2) application of the evident fusion rules. Fig. 6 illustrates the overall process.

(1) Fuzzy matter element (FME) method for BPAs

The construction of BPAs is a challenging problem in the application of D-S evidence theory. There is a fuzzy correlation between the multi-source heterogeneous risk factor measures involved in the construction process. For example, the experience and status of different workers affects the risks of mechanical operation; and different mechanical operation methods and other factors affect the risks of the construction process. However, the correlation is uncertain and is difficult to evaluate with traditional data analysis methods. In order to solve the incompatibility problems with traditional methods, a fuzzy matter element method was adopted to construct the BPAs in the new method and system.

FME is a data processing method based on the fuzzy set theory and the matter element analysis theory [53]. FME describes the nature of things objectively and accurately through the correlation function from both the qualitative and quantitative aspects and explicitly explains the intrinsic relationship between the matter and the quantity of the matter, as well as the law of its changes. It shows the fuzziness and incompatibility during the process of information expression, acquisition, and reasoning, and has been regarded as an effective method for multi-factor evaluation. Yin [54] showed that FME was able to solve the problem of contradictory mathematical functions and constraint conditions and pointed out that by combining qualitative and quantitative models, the multi-objective negotiation problem can be transformed into a single-objective consultation problem. Sheng [55] and Qi [56] discussed the basic principles of using FME to define mass functions in D-S evidence theory and demonstrated its use for multi-source data fusion. Scholars have achieved good results applying FME to evaluate multi-factor indices in fields such as complex project safety assessment [57,58].

In FME, the matter-element model $S = (A, C, X)$ is defined as a three–element set, where A is the matter element, C is the feature of A, and X is the value of C. C reflects one specific aspect of a matter element A, thus A could have multiple features such as C_1, C_2, …, C_N, which have corresponding values of x_1, x_2, …, x_N, where n is the number of features. S_N is called a N dimension matter element, which is defined as Eq. (3)

$$S_N = [A, C, X] = \begin{bmatrix} A & C_1 & x_1 \\ & C_2 & x_2 \\ & \vdots & \vdots \\ & C_N & x_N \end{bmatrix} \tag{3}$$

where $C_i(i = 1, 2, \ldots, N)$ is the ith feature of A, and $x_i(i = 1, 2, \ldots, N)$ is the value of C_i, which, in this case, is the index data of the object to be evaluated.

For specific objects, the matter element A can be further discretized into different states according to the actual requirements. In risk assessment, particularly, it is very important to define different standards under different risk conditions. For example, the severity of a risk can be classified into five grades: I, II, III, IV, and V, from light to heavy. In this sense, if a matter element A is divided into M discrete states, the measurement of X in different states becomes a fuzzy problem. Therefore, S_{NM} is called the fuzzy N-dimensional matter element, as defined in Eq. (4).

$$S_{NM} = \begin{bmatrix} & \mathrm{A}_1 & \mathrm{A}_2 & & \mathrm{A}_M \\ C_1 & f_{11}(x_1) & f_{12}(x_1) & \ldots & f_{1M}(x_1) \\ C_2 & f_{21}(x_2) & f_{22}(x_2) & \ldots & f_{2M}(x_2) \\ \vdots & \vdots & \vdots & & \vdots \\ C_N & f_{N1}(x_N) & f_{N2}(x_N) & \ldots & f_{NM}(x_N) \end{bmatrix} \tag{4}$$

where S_{NM} is a N-dimensional fuzzy matter element; $C_i(i = 1, 2, \ldots, N)$ is the ith feature of the matter element, $x_i(i = 1, 2, \ldots, N)$ is the value of the evaluation index C_i, that is, the index data of the object to be evaluated;A_j is the jth ($j = 1, 2, \ldots, M$) state of the matter-element; $f_{ij}(x_i)$ ($i = 1, 2, \ldots, N$; $j = 1, 2, \ldots, M$) is the fuzzy membership of the ith feature C_i in the jth state.

Considering multiple variables $C_i(i = 1, 2, \ldots, N)$ that are involved during construction, the perception of risk is a multi-objective decision-making problem with discrete sample spaces and discrete observable

random variables. Since index factors are discrete, they can be further divided into different states $\{A_1, A_2, \ldots, A_M\}$ by fuzzification, which converts a brittle value into the membership degree of a fuzzy set. In this paper, each state $A_j (j = 1, 2, \ldots, M)$ corresponds to a specific closed interval. The input multi-sensor data are converted into a series of values between 0 and 1 to represent their membership degrees, calculated using Eq. (5).

$$f_{ij}(x_i) = \exp\left[-\left(\frac{x_i - a_{ij}}{b_{ij}}\right)^2\right] \tag{5}$$

where $f_{ij}(x_i)$ is the fuzzy membership of x_i for the ith feature C_i in the jth state, x_i is a specific number of the ith index factor, and a_{ij} and b_{ij} are constant values of FEM function, calculated using Eqs. (6) and (7).

$$a_{ij} = \frac{x_{ij}(L) + x_{ij}(R)}{2} \tag{6}$$

$$b_{ij} = \frac{x_{ij}(R) - x_{ij}(L)}{3} \tag{7}$$

where $x_{ij}(L)$ and $x_{ij}(R)$ are the lower and upper bounds of the ith feature C_i in the jth state.

Following the calculations through Eqs. (5) through (7), the relationship between x_i and A_i is obtained as the fuzzy membership degree and is then used to construct the BPAs of influencing factors C_i. Eq. (8) illustrates the computation of BPAs.

$$\begin{cases} m_i(A_j) = f_{ij}(x_i) \\ m_i(\Theta) = 1 - \sum_{j=1}^{N} m_i(A_j) \end{cases} \tag{8}$$

where $m_i(A_j)$ is the BPA of A_j, and $m_i(\Theta)$ is the value of the uncertain state of C_i, which means no focal element can be determined in this state and thus all sub-units are included.

(2) Evidence fusion method mixed with FME

The purpose of evidence fusion rules mixed with FME is to discretize the collection of evidence into non-overlapping sets. The hybrid fusion rule is adopted to fuse the multi-source evidence body by independent judgement of the recognition framework of D-S evidence theory. This framework is as follows.

Viewing any object as a system, if Θ is the recognition framework of the system, then $\Theta = \{\theta_1, \ldots, \theta_M\}$. If set function $m: 2^{\theta} \rightarrow [0, 1]$, where 2^{θ} is the power set of Θ, satisfies the following conditions:

(1) $\sum_{A \subseteq \Theta} m(A) = 1$,

(2) $m(\varnothing) = 0$, $\varnothing$ is an empty set.

then for $\forall A \in 2^{\Theta}$, $m(A)$ is called the *mass* function or BPA of A. $m(A)$ reflects the extent to which evidence body supports A, but not any particular subsets of A, and thus indicates the exact reliability of A itself. $m(\Theta)$ is called the uncertainty of A. Any $A \in 2^{\Theta}$ that satisfies $m(A) > 0$ is called a Focal Element, and the union of all focal elements is called the core of evidence.

In order to integrate information more effectively, D-S evidence theory builds up a series of *mass* functions and fuses multi-source information through the Dempster rules. The Dempster rules of two evidence bodies are defined as Eq. (9).

$$\begin{cases} m_{1,2}(A) = \begin{cases} \frac{1}{1 - K_{1,2}} \sum_{A_i \cap A_j = A \neq \varnothing} m_1(A_i) m_2(A_j), \ \forall A \subseteq \Theta, A \neq \varnothing \\ 0, A = \varnothing \end{cases} \\ K_{1,2} = \sum_{A_i \cap A_j = \varnothing} m_1(A_i) m_2(A_j) \end{cases} \tag{9}$$

where $m_1(A)$ and $m_2(A)$ are two *mass* functions under the same recognition framework, $m_{1,2}(A)$ is the fusion result of two *mass* functions, and $K_{1,2}$ is the conflict between two evidence bodies.

Despite the advanced performance in reasoning with uncertainties, the traditional Dempster rule has inevitable shortcomings in fusing evidence of high conflict, which are often counterintuitive. To be specific, the conflict coefficient K from Eq. 9 is a value less than 1; however, when the conflict coefficient K approaches very close to 1, the Dempster rule will lead to the anti-intuition problem [59]. When $K_{1,2} = 1$, the evidence bodies have a complete conflict, which means the failure of Dempster rule.

In order to solve the counter-intuitive problem, the new method and system in this paper adopted a mixed evidence fusion rule. As shown in Fig. 4, a threshold ξ is set to detect conflict of evidence. If a high conflict is detected, a weighted average rule will be implemented to fuse high conflict evidences, otherwise the Dempster rules will be used for evidence fusion. The weighted average rule is defined as Eq. (10).

$$\begin{cases} m(A) = \sum_{o=1}^{O} (\omega_0 \times m_0(A)) \\ \omega_0 = \begin{cases} \frac{1}{O}, & d_0 = 0 \\ \frac{1/d_0}{\sum_{o=1}^{o=O} 1/d_0}, & d_0 \neq 0 \end{cases} \\ d_0 = \sum_{i=1}^{i=O} \sqrt{\sum_{j=1}^{j=M} (m_0(A_j) - m_i(A_j))^2} \end{cases} \tag{10}$$

where ω_0 is the weight of the oth evidence body in fusion, and d_0 is the total Euclidian distance between the oth evidence body and the others.

The value of the threshold ξ depends on the application of practical projects. Since this new method and system focuses on risk perception and evaluation during undersea tunneling, considering the fused multi-source information mainly comes from sensors and 5% is a common acceptable error rate in practice, the value of ξ is set at 0.95. When K is less than 0.95, the Dempster rule is used, and when K is greater than or equal to 0.95, the weighted average rule is used.

3.3. BIM module

As the project progresses, the quality information is collected and organized through the 4M1E–WBS module and fused through the risk assessment module to compute the risk indices. The results are sent to the BIM module for storage, management, and visualization. The BIM platform also contains a database of risk assessments from previous projects and a collection of risk solutions. Note that this database of risk assessment information of previous projects grows continuously (i.e., the results of the current project are saved and become a part of the database for reference on future projects). Each risk index is compared with previous experiences in the database to determine if an action needs to be taken to control the risk, and such actions are retrieved from the database of risk solutions. Fig. 7 illustrates a scenario where not only the segment where the risk occurs, but also the level of the risk, the components where the risk exists, and the factors that cause the risk are displayed. This feature greatly facilitates the retrieval of quality information for each construction section and enables managers to perceive risk and then communicate solutions and actions to the whole team in real-time.

4. Case study and illustration

4.1. Case study background

The shield cutter accident during the Xiamen Metro Line No. 3 project was utilized to test the new method and system due to the complexity and severity of the accident. Metro Line No. 3 is an undersea tunnel located between Wuyuan Wan Station and Liuwu Dian Station in Xiamen, China. The whole line was successively divided into three

Fig. 7. Risk visualization in BIM.

sections: 1) the EPB section, 2) the mining method section, and 3) the SS section. The EPB section is 871 m long and mainly crossed land. The SS section is 1419 m long, of which 1159 m crossed the sea with the remainder crossing land (Fig. 8). The two main challenges in this construction project were the complexity of the geology and the direct connection of the underground water to seawater. From the aspect of geology, the upper layer was relatively soft while the lower layer was harder and full of bedrock bulges, boulders, weathered slots, and severely mantled rocks, which made the shield machine's work very difficult. The connection of underground water to seawater made the construction process extremely vulnerable to collapses.

The shield cutter accident in question happened on the left 343 rings (K18 + 836.94–K18 + 838.41) during the construction process. This accident was classified as the highest-grade risk according to the *Code for Risk Management of Underground Works in Urban Rail Transit* [66]. The details of the accident are as follows:

1) At an early stage, the early-warning system of the shield cutter failed to work and triggered an alarm. On-site repair was not accessible due to the weathered geologic condition and the project manager decided to continue the work without repair.

2) Unknown obstacles were encountered at a place which the geologic exploration had reported as a “fully weathered area.” The obstacles caused a sharp wear to the cutter and sent the cutter deep into the soil.

3) The direct removal or replacement of the cutter on the site was not feasible due to the loose soil and bubbling sea floor, which posed a great danger of causing a backwash of the seawater. As a solution, a freezing method was used to handle the broken cutter and led to a direct economic loss of up to 22 million RMB and a half-year delay in the project.

This accident was used as the case study to illustrate the functionality of the new method and system.

4.2. Case risk assessment calculation

To test the new method and system, the relevant quality data immediately preceding the accident were collected and are summarized in Table 4. The indicator number (I N) is the same number shown in Tables 1 and 2.

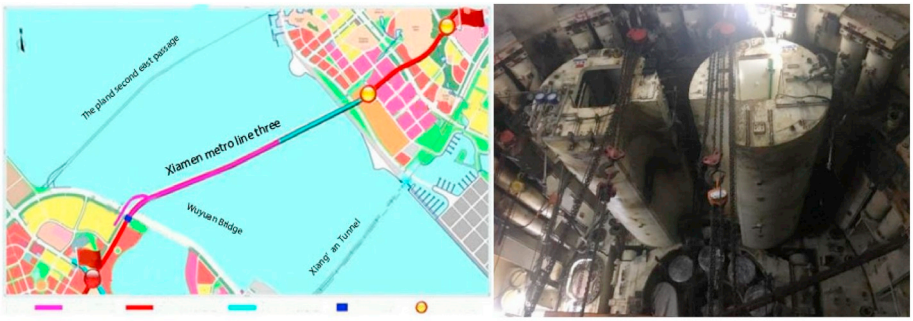

(a) Sections of Xiamen Metro Line 3 **(b) Shield Machine Disassembly**

Fig. 8. Background Information of the Case Study
(a) Sections of Xiamen Metro Line 3
(b) Shield Machine Disassembly.

Table 4
Quality data at Wuyuan bay construction site.

I N[a]	Measured value	Normalized value	C R[b]	I N[a]	Measured value	Normalized value	C R[b]
C_1	76	0.506	I	C_{25}	0.04	0.4	III
C_2	0.6	0.7	IV	C_{26}	0	0	I
C_3	2	0.90	V	C_{27}	0	0	I
C_4	2	0.90	V	C_{28}	10	0.1	I
C_5	6	0.70	III	C_{29}	−1	0.01	I
C_6	3.4	0.068	I	C_{30}	26	0.26	II
C_7	1405	0.281	II	C_{31}	0	0	I
C_8	2.80	0.112	I	C_{32}	−2	0.25	III
C_9	0.19	0.380	II	C_{33}	4	0.5	IV
C_{10}	206	0.412	III	C_{34}	19.00	0.525	II
C_{11}	0	0	I	C_{35}	3.167	0.367	I
C_{12}	8	0.320	II	C_{36}	6	0.24	I
C_{13}	0.05	0.10	I	C_{37}	1	0	I
C_{14}	0.16	0.32	II	C_{38}	5.86	0.234	II
C_{15}	0.04	0.08	I	C_{39}	24.3	0.243	II
C_{16}	15	1	V	C_{40}	0.769	0.338	II
C_{17}	25	1	V	C_{41}	38	0.62	IV
C_{18}	25	1	V	C_{42}	−0.07	0.215	I
C_{19}	1	1	V	C_{43}	5.84	0.883	IV
C_{20}	2.9	0.033	I	C_{44}	0.488	0.104	I
C_{21}	3.7	0.26	II	C_{45}	0.108	0.892	V
C_{22}	0	0	I	C_{46}	0	1	V
C_{23}	0	0	I	C_{47}	12.5	0.875	V
C_{24}	5	0.5	III	C_{48}	15	0.75	V

[a] Indicator number.
[b] Classification result.

4.2.1. Construction of BPAs

The BPAs were calculated for each index factor using Eqs. 5 through 8, and the results are shown in Table 5.

4.2.2. Fusion results of risk indices

Table 6 illustrates the fusion results for the risk factors under the (hu)man category and the fused risk classification at the category level. Tables 7, 8, 9, and 10 illustrate the fusions results for the machine, material, method, and environment categories, respectively.

4.2.3. Fusion result of the overall risk

Previous studies [61,62] have shown that 80–90% of tunneling accidents are attributable to unsafe (hu)man behavior, construction equipment, and the work environment. Therefore, in this study, the fusion results of the (hu)man, machine, and environment factors were integrated utilizing D-S theory as well as the material and method fusion results. The weights for the man-machine-environment risks and the material-method risks were set at 90% and 10%, respectively. The fusion process is described below, and the fusion results of the overall risk of the shield cutter accident are shown in Table 12. The results suggest a Class V risk (the highest risk group), which aligns with the reality (i.e., an accident actually occurred).

4.3. Analyses of results and observations

The overall risk prior to the occurrence of the accident was assessed as Class V (the highest risk). For the five main categories, the risk for the (hu)man category was assessed as Class IV, the machine category risk was Class V, the method category also was Class V, the method category was Class I, and the environment category was Class V.

The following observations were made from the data relevant to this accident. 1) The fourth-level risk (Class IV) of the (hu)man category was caused by a lack of work and technical experience as well as management skills in undersea shield tunneling. 2) The fifth-level risk (Class V) of the machine category occurred for two main reasons: a) when the alarm system of the shield cutter failed, a timely repair was not provided; and b) unknown obstacles caused severe damage to the cutter, which was the direct result of the false geologic report and the failed alarm system. 3) The fifth-level risk (Class V) of the environment category was due to the complex geology of the site, which posed danger to on-site repairs as it could have easily caused a severe salt-water encroachment. The main causes were traced to the (hu)man category risk factors. If the team had possessed the necessary skills, knowledge, and experience, they would have made timely decisions prior to the accident to prevent its occurrence and timely repairs would

Table 5
Construction of BPAs.

Indicator		BPAs					
		$m(A_1)$	$m(A_2)$	$m(A_3)$	$m(A_4)$	$m(A_5)$	$m(\Theta)$
(hu)Man	C_1	0.179	0.003	0.000	0.000	0.000	0.818
	C_2	0.000	0.000	0.000	1.000	0.000	0.000
	C_3	0.000	0.000	0.000	0.000	0.779	0.221
	C_4	0.000	0.000	0.000	0.000	0.779	0.221
	C_5	0.000	0.000	0.445	0.000	0.000	0.555
Machine	C_6	0.794	0.000	0.000	0.000	0.000	0.206
	C_7	0.001	0.992	0.000	0.000	0.000	0.007
	C_8	0.968	0.000	0.000	0.000	0.000	0.032
	C_9	0.000	0.237	0.039	0.000	0.000	0.724
	C_{10}	0.000	0.060	0.175	0.000	0.000	0.765
	C_{11}	1.000	0.000	0.000	0.000	0.000	0.000
	C_{12}	0.000	0.914	0.001	0.000	0.000	0.085
	C_{13}	1.000	0.000	0.000	0.000	0.000	0.000
	C_{14}	0.000	0.914	0.001	0.000	0.000	0.085
	C_{15}	1.000	0.000	0.000	0.000	0.000	0.000
	C_{16}	0.000	0.000	0.000	0.000	1.000	0.000
	C_{17}	0.000	0.000	0.000	0.000	1.000	0.000
	C_{18}	0.000	0.000	0.000	0.000	1.000	0.000
	C_{19}	0.000	0.000	0.000	0.000	1.000	0.000
Material	C_{20}	1.000	0.000	0.000	0.000	0.000	0.000
	C_{21}	0.003	0.698	0.000	0.000	0.000	0.299
	C_{22}	1.000	0.000	0.000	0.000	0.000	0.000
	C_{23}	1.000	0.000	0.000	0.000	0.000	0.000
Method	C_{24}	0.000	0.000	1.000	0.000	0.000	0.000
	C_{25}	0.000	0.106	0.106	0.000	0.000	0.788
	C_{26}	1.000	0.000	0.000	0.000	0.000	0.000
	C_{27}	1.000	0.000	0.000	0.000	0.000	0.000
	C_{28}	1.000	0.000	0.000	0.000	0.000	0.000
	C_{29}	1.000	0.000	0.000	0.000	0.000	0.000
	C_{30}	0.003	0.698	0.000	0.000	0.000	0.299
	C_{31}	1.000	0.000	0.000	0.000	0.000	0.000
	C_{32}	0.000	0.106	0.105	0.000	0.000	0.789
	C_{33}	0.000	0.000	0.105	0.105	0.000	0.790
	C_{34}	0.000	0.018	0.018	0.000	0.000	0.964
	C_{35}	0.208	0.019	0.000	0.000	0.000	0.773
	C_{36}	0.317	0.002	0.000	0.000	0.000	0.681
	C_{37}	1.000	0.000	0.000	0.000	0.000	0.000
Environment	C_{38}	0.018	0.376	0.000	0.000	0.000	0.606
	C_{39}	0.010	0.482	0.000	0.000	0.000	0.508
	C_{40}	0.000	0.723	0.003	0.000	0.000	0.274
	C_{41}	1.000	0.000	0.000	0.000	0.000	0.000
	C_{42}	0.311	0.004	0.000	0.000	0.000	0.685
	C_{43}	0.000	0.000	0.000	0.990	0.000	0.010
	C_{44}	0.000	0.000	0.001	0.375	0.018	0.606
	C_{45}	0.000	0.000	0.000	0.011	0.647	0.342
	C_{46}	0.000	0.000	0.000	0.000	1.000	0.000
	C_{47}	0.000	0.000	0.000	0.000	1.000	0.000
	C_{48}	0.000	0.000	0.000	0.000	1.000	0.000

Table 6
Information fusion decision results of (hu)man factors.

Category	Grade					$m(\Theta)$	Fusion results
	$m(A_1)$	$m(A_2)$	$m(A_3)$	$m(A_4)$	$m(A_5)$		
Worker	0.000	0.000	0.000	1.000	0.000	0.000	IV
Technician	0.000	0.000	0.000	0.000	0.779	0.221	V
Manager	0.000	0.000	0.445	0.000	0.000	0.555	–
(hu)Man	0.000	0.000	0.000	1.000	0.000	0.000	IV

Table 7
Information fusion decision results of machine.

Category	Grade					$m(\Theta)$	Fusion results
	$m(A_1)$	$m(A_2)$	$m(A_3)$	$m(A_4)$	$m(A_5)$		
Shield machine parameters	0.459	0.536	0.001	0.000	0.000	0.004	II
Shield tail brush protection	1.000	0.000	0.000	0.000	0.000	0.000	I
Mud water comprehensive management system	1.000	0.000	0.000	0.000	0.000	0.000	I
Tool disk wear	0.000	0.000	0.000	0.000	1.000	0.000	V
Mechanical failure	0.000	0.000	0.000	0.000	1.000	0.000	V
Machine	0.000	0.000	0.000	0.000	1.000	0.000	V

Table 8
Information fusion decision results of material.

Category	Grade					$m(\Theta)$	Fusion results
	$m(A_1)$	$m(A_2)$	$m(A_3)$	$m(A_4)$	$m(A_5)$		
Grouting material	1.000	0.000	0.000	0.000	0.000	0.000	I
Mud water material	1.000	0.000	0.000	0.000	0.000	0.000	I
Material	1.000	0.000	0.000	0.000	0.000	0.000	I

Table 9
Information fusion decision results of the method.

Category	Grade					$m(\Theta)$	Fusion results
	$m(A_1)$	$m(A_2)$	$m(A_3)$	$m(A_4)$	$m(A_5)$		
Geological exploration	0.000	0.000	1.000	0.000	0.000	0.000	III
Cut water pressure	0.000	0.106	0.106	0.000	0.000	0.788	–
Synchronous grouting	1.000	0.000	0.000	0.000	0.000	0.000	I
Shield posture	1.000	0.000	0.000	0.000	0.000	0.000	I
Shield trend	0.000	0.087	0.183	0.086	0.000	0.644	–
Tunnel design	1.000	0.000	0.000	0.000	0.000	0.000	I
Method	1.000	0.000	0.000	0.000	0.000	0.000	I

Table 10
Information fusion decision results of the environment.

Category	Grade					$m(\Theta)$	Fusion results
	$m(A_1)$	$m(A_2)$	$m(A_3)$	$m(A_4)$	$m(A_5)$		
Sea water	0.018	0.376	0.000	0.000	0.000	0.606	–
Soil	0.382	0.000	0.000	0.614	0.000	0.004	IV
Rock	0.000	0.000	0.000	0.000	1.000	0.000	V
Environment	0.194	0.001	0.000	0.303	0.500	0.002	V

Table 12
Decision fusion of risk state for cutter head accident of shield machine.

The accident risk of shield machine cutter

$$= (0.9\ \ 0.1)\begin{pmatrix} 0.000 & 0.000 & 0.000 & 0.378 & 0.622 & 0.000 \\ 1.000 & 0.000 & 0.000 & 0.000 & 0.000 & 0.000 \end{pmatrix}$$
$$= (0.100\ \ 0.000\ \ 0.000\ \ 0.340\ \ 0.560\ \ 0.000)$$

$m(A)$	Grade					$m(\Theta)$	Fusion results
	$m(A_1)$	$m(A_2)$	$m(A_3)$	$m(A_4)$	$m(A_5)$		
Man-machine-environment	0.000	0.000	0.000	0.378	0.622	0.000	V
Material-method	1.000	0.000	0.000	0.000	0.000	0.000	I
4M1E	0.100	0.000	0.000	0.340	0.560	0.000	V

have been made when the shield machine was damaged. For that reason, more attention should be paid to risk control in the (hu)man category factors.

The new method and system produced the same result as the actual risk level for the shield cutter accident that occurred during the Xiamen Metro Line No. 3 project, which proves the feasibility of using improved D-S evidence fusion theory in risk assessment for undersea tunneling. The implementation of this new system fills the dynamic risk assessment gap of existing risk management methods and will help practitioners assess their risks in real-time during the construction process and thereby avoid financial losses as well as project delays caused by accidents.

5. Discussion

The new method and system presented in this paper could be universally implemented for undersea tunnel shield construction projects in different cities and different countries or in different sections of the same project. Generally, this method and system can be used by adding or defaulting some factors according to actual situations, and implementation is expected to be easier than for the Xiamen case. For the default factors, if they will not be in the final fusion, the default values will not affect the evaluation results. If the default factors are incorporated in the final fusion, there are three methods to enable their use: 1) fill in the predicted value; 2) copy the last valid value; or 3) if 1) and 2) are not possible, fill in the median value. According to the 4M1E grading system in this new method and system, the dynamic indices of (hu)man, machine, materiel, method, and environment for different projects can be obtained through the 4M1E-WBS module, which serves as the pre-input parameters of the fusion algorithm whereby accurate risk assessment of undersea tunnel shield construction in different regions can be achieved.

However, there are two limitations in the proposed method and system. First, it could not realize real-time data acquisition and risk dynamic interaction. Risk is by nature dynamic and interdependent [63]. While in our study we did consider risk influence to a certain extent, this is an area that would greatly benefit from further efforts to model and simulate risk interactions to more accurately model the risk interaction and assess the overall risk at the project level. Second, the risk response strategy is still a textual database of predesigned strategies. An updated mechanism is lacking that could substantiate the database with more versatile strategies as well as lessons learned from past experience. Efforts in this regard would advance the validity of the new method's results.

The validity and applicability of the new method and system was verified by the construction rings overall line 3. Quality measurement data were obtained from the site for the randomly selected construction sections of the 827th–834th rings and 907th–912th rings from the shield section between Wuyuan Wan Station and Liuwu Dian Station. The overall construction risk index was determined following the fusion process: fusing risk measures – the third level risk indicators – leads to the risk indices of the risk factors – the second level risk indicators, fusing the second level risk indices leads to the risk indices of the risk

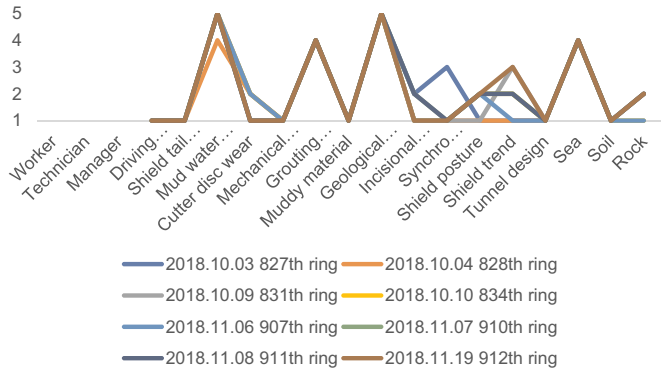

Fig. 9. Grade change of secondary index.

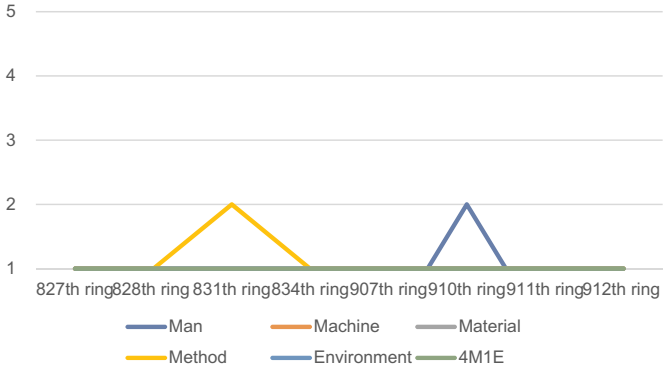

Fig. 10. Grade change of categories.

categories of 4M1E – the first level risk indicators, and finally fusing the first level risk indices to determine the overall construction risk. Fig. 9 illustrates the risk indices of the second level risk indicators. Attributed to the variations in the values of third level risk indicators, the fusion results show fluctuations. For example, the fusion result for the secondary index of "mud water management system" in the 912th ring is in the range of grade V, but the fusion results for both the secondary indices of "cutter disc wear" and "mechanical failure" are in grade I. Fig. 10 illustrates the risk indices of the first level risk indicators, or the five categories of 4M1E, and the overall risk. Other than the method risk index of the 831th ring and the man risk index of the 910th ring being in grade II, all the first level risk indices and the overall risk index were in grade I. The calculation results show that the overall risk levels were all Class I, and no construction accidents occurred at the construction sites from October 2018 to mid-November 2018. The multi-source information fusion method was consistent with the actual situation.

The new method and system were found to be practical for underground tunnel risk management. At present, a Xiamen Metro Line 3 construction risk management system is being developed and the core algorithm has been tested. The results are in good agreement with the actual situation, which greatly assists the subway construction risk management team. This new multi-source integrated assessment method and system for undersea tunnel construction risk is a universal method integrating data collection, risk assessment, and BIM risk management. This system can store multiple engineering sections by setting index system parameters according to the actual situation of projects in different regions and calculating the risk level, can provide real-time visualization of construction risks, and can quickly locate the sections, processes, and positions where construction risks occur that are needed to carry out unified management and avoid construction risks to the greatest extent. Therefore, this new method and system can be used for other underground tunnel construction technologies and building construction types, with the only additional work needed being determination of the appropriate evaluation factor for the project according to the 4M1E framework and building the BIM models.

6. Summary and conclusions

A new construction risk assessment method and system based on 4M1E multi-source information fusion was presented in this paper to solve the problems of subjectivity and static evaluation in risk assessment and management in undersea tunneling projects. First, the relationship between the quality and the risk was established using the 4M1E categories as the bridge to integrate the quality and risk measures so that risk could be better quantified by deterministic quality measures. Using D-S evidence theory and FME, the quality data were stratified and fused to avoid the subjectivity in the current expert scoring practices to assess risk. The new method and system were implemented on a BIM platform for integrated quality and risk management to take advantage of the merits of BIM in information modeling, data management, and visualization. The resulting BIM database collects not only the risk information of a specific project but also retains the risk information from past projects and potential solutions. As such, it not only visualizes where the risks are, but also provides guidance on actions to take when encountering risks as a project progresses. The new method and system was tested and validated using a construction safety case study of a shield cutter accident that occurred during the Xiamen Metro Line No. 3 project. An empirical analysis was conducted to verify the effectiveness of the method; and the results show that the overall risk was at the highest level (i.e., Class V) prior to the accident.

Future work will focus on four main avenues of research. 1) Sensing tools for real-time data acquisition. We will pursue sensors that not only use radio frequency identification (RFID), LiDAR, cameras and camcorders, and fiber bragg grating (FBG), but also innovative new sensors that can sense factors which heretofore were either ineffectively perceived or not at all. 2) Real-time monitoring and control. Multi-sensor systems and leveraging advances in cyber-physical systems (CPS) and the Internet of Things (IoT) will be pursued to provide dynamic response and automatic control. 3) Mechanisms for updating the stratagem database. We are working on "lessons learned" from past experience, which will be published in future papers. 4) Finally, we fully realize that the interactions between risk factors is a puzzle problem, and it will take a long time to develop an algorithm that is better than the D-S theory algorithm for precise evaluation of construction risk.

Acknowledgement

This research was supported by the National Natural Science Foundation of China (Grant No. 71871192), the China Railway South Investment Group Co. LTD., Major Science and Technology Planning 2016 "Xiamen Metro No. 3 Line Undersea Tunnel Construction Risk Integrated Control and System Development" and "Xiamen Engineering Technology Center for Intelligent Maintenance of Infrastructures" (No. TCIMI201802).

Declaration of competing interest

There is no conflict of interest in this research.

Appendix A. Appendix

Our detailed procedures for calculating the risk level of undersea tunnel construction using improved D-S evidence theory are listed here, taking

the case study in this paper as an example.

1) Risk index classification of undersea tunnel shield construction method
2) Normalized measured multi-source data

The above steps are elaborated in Tables 2 and 3 in the text, and the normalized value of the relevant quality data immediately preceding the accident are listed in Table 4 in the text.

3) Construction of BPAs

Eqs. 5 through 8 in the text are used to calculate the BPAs of each index factor, BPA construction process of C_1 (average heart rate of workers) indicator is as follows:

According to formula 6 and 7, constants a and $b$of FEM function are calculated:

$$a_{11} = \frac{x_{11}(L) + x_{11}(R)}{2} = \frac{0 + 0.54}{2} = 0.27$$

$$b_{11} = \frac{x_{11}(R) - x_{11}(L)}{3} = \frac{0.54 - 0}{3} = 0.18$$

According to Eq. (5), the membership function of FME is:

$$f_{11} = \exp\left[-\left(\frac{x_1 - a_{11}}{b_{11}}\right)^2\right] = \exp\left[-\left(\frac{0.506\text{-}0.27}{0.18}\right)^2\right] = 0.179$$

According to Eq. (8), the BPAs of A can express as $m_i(A_j) = f_{ij}(x_i)$, then

$$m_1(A_1) = f_{11}(x_{11}) = 0.179$$

Similarly, the BPAs of A in C_1 index are calculated as follows:

$m_1(A_2) = 0.003$ $m_1(A_3) = 0.000$

$m_1(A_4) = 0.000$ $m_1(A_5) = 0.000$

According to Eq. (8), BPA value with uncertain size of C_1 index is

$$m_1(\Theta) = 1 - \sum_{j=1}^{5} m_1(A_j) = 0.818$$

In particular, if the measured value is less than the median of the first interval or greater than the median of the fifth interval, BPA is assigned a value of 1 at the corresponding interval and 0 at the other intervals. Similarly, BPAs were constructed for other indices and the results are shown in Table 5 in the text.

4) Index factors fusion

Taking information fusion decision of (hu)man as an example:

The BPAs of C_1, C_2 and C_3 can be obtained from Table 13 as follows:

Table 13
The BPAs of indicators C_1, C_2 and C_3.

Indicator	BPAs					
	$m(A_1)$	$m(A_2)$	$m(A_3)$	$m(A_4)$	$m(A_5)$	$m(\Theta)$
C_1	0.179	0.003	0.000	0.000	0.000	0.818
C_2	0.000	0.000	0.000	1.000	0.000	0.000
C_3	0.000	0.000	0.000	0.000	0.779	0.221

The fusion process of mean heart rate (C_1) and the nearest position to the hazard source (C_2) is as follows:

According to Eq. (9):

$$K_{1,2} = \sum_{A_i \cap A_j = \varnothing} m_1(A_i) m_2(A_j) = 0.182 < 0.95$$

Complied with the D-S rule, then

$$m_{1,2}(A_1) = \frac{1}{1 - K_{1,2}} \sum_{A_i \cap A_j = A \neq \varnothing} m_1(A_i) m_2(A_j),\ \forall\ A \subseteq \Theta,\ A \neq \varnothing$$

$$= \frac{0.179 \times 0.000 + 0.179 \times 0.000 + 0.000 \times 0.818}{1 - 0.182} = 0$$

Similarly, $m_{1,\ 2}(A_2) = 0$, $m_{1,\ 2}(A_3) = 0$, $m_{1,\ 2}(A_4) = 1$, $m_{1,\ 2}(A_5) = 0$, continue to fuse fusion results of C_1 and C_2 indicators with C_3 indicators,

$$K_{1,2,3} = \sum_{A_i \cap A_j = \varnothing} m_{1,2}(A_i) m_3(A_j) = 0.779 < 0.95$$

$$m_{1,2,3}(A_1) = \frac{1}{1 - K_{1,2,3}} \sum_{A_i \cap A_j = A \neq \varnothing} m_{1,2}(A_i) m_3(A_j), \forall A \subseteq \Theta, A \neq \varnothing$$

$$= \frac{0.000 \times 0.000 + 0.000 \times 0.221 + 0.000 \times 0.000}{1 - 0.779} = 0$$

Similarly, $m_{1,2,3}(A_2) = 0$, $m_{1,2,3}(A_3) = 0$, $m_{1,2,3}(A_4) = 1$, $m_{1,2,3}(A_5) = 0$.

That is, the fusion results of the worker indicator. Fuse the third grade indices in turn, and then getting the risk results of the worker, the technician, and the manager, and then fusing the three second-level indices to get the (hu)man risk level. The result of the fusion decision of (hu)man factor is shown in Table 6 in the text. Similarly, the fusion results of other first-level indicators are obtained, shown in Tables 7 through 10 in the text. The overall risk level calculation method is shown in Section 4.2 in the text.

References

[1] C. Yuan, J. Park, X. Xu, H. Cai, D.M. Abraham, M.D. Bowman, Risk-based prioritization of construction inspection, Transportation Research Records. 2672 (26) (2018) 96–105, https://doi.org/10.1177/0361198118782025.

[2] J.R. Ribas, M.E. Arce, F.A. Sohler, A. Suarez-Garcia, Multi-criteria risk assessment: case study of a large hydroelectric project, Cleaner Production. 227 (1) (2019) 237–247, https://doi.org/10.1016/j.jclepro.2019.04.043.

[3] X. Zhao, B.G. Hwang, S.P. Low, An enterprise risk management knowledge-based decision support system for construction firms, Eng. Constr. Archit. Manag. 23 (3) (2016) 369–384, https://doi.org/10.1108/ECAM-03-2015-0042.

[4] J. Yuan, Q. Zhang, Theory and Application of Total Project Management, GeoHunan International Conference 2009, Changsha, Hunan, China, 190 ASCE Publications, 2009, p. 116, https://doi.org/10.1061/41042(349)15.

[5] J. Liu, F. Guo, Construction quality risk management of projects on the basis of rough set and neural network, Computer Modelling & New Technologies 18 (11) (2014) 791–797 https://pdfs.semanticscholar.org/02d2/713bcc0a01ee9cffd868fc73ce63a684ae9d.pdf.

[6] X. Wu, Y. Wang, L. Zhang, L. Ding, M.J. Skibniewski, J. Zhong, A dynamic decision approach for risk analysis in complex projects, Journal of Intelligent & Robotic Systems 79 (3) (2015) 591–601, https://doi.org/10.1007/s10846-014-0153-3.

[7] P. Haize, M. Wei, H. Jian, The seepage risk assessment of shield tunnel on the basis of intuitionistic fuzzy entropy theory, Electronic Journal of Geotechnical Engineering 21.13 (2016) 4101–4119 http://www.ejge.com/2016/Ppr2016.0406ma.pdf.

[8] W. Liu, T. Zhao, W. Zhou, J. Tang, Safety risk factors of metro tunnel construction in China: an integrated study with EFA and SEM, Saf. Sci. 105 (2018) 98–113, https://doi.org/10.1016/j.ssci.2018.01.009.

[9] Y. Yang, J. Wang, G. Wang, Y.W. Chen, Research and development project risk assessm-ent using a belief rule-based system with random subspaces, Knowledge-Based System. 178 (2019) 51–60, https://doi.org/10.1016/j.knosys.2019.04.017.

[10] M. Popescu, L.U.A. Dasc, Considerations on integrating risk and quality management, Annals of Dunărea De Jos University Fascicle I Economics and Applied Informatics 1 (1) (2011) 49–54 http://www.arthra.ugal.ro/bitstream/handle/123456789/805/ugal_f1_2011_nr1_6_Popescu_Dascalu.pdf?sequence=2&isAllowed=y.

[11] Q. Shen, Research on the Integration of Construction Quality Factors and Risk Management Based on BIM—Taking Xiamen Subway Line Three Cross-sea Tunnel as an Example (Master Thesis), Department of Architecture and Civil Engineering, Xiamen University, 2018, https://kns.cnki.net/KCMS/detail/detail.aspx?dbcode=CMFD&dbname=CMFD201902&filename=1018195542.nh&uid=WEEvREdxOWJmbC9oM1NjYkZCbDdrNTBKanc1Z2gxUklEMW5hYmpTNS9pcVc=$R1yZ0H6jyaa0en3RxVUd8dfoHi7XMMDo7mtKT6mSmEvTuk11l2gFA!!&v=MTk5OTBUSXJaRWJQSVI4ZVgxTHV4WVM3RGgxVDNxVHJXTTFGckNVUkxPZVp1ZHRGaW5uVkx2S1ZGMjZGckt4Rzk=.

[12] https://www.vjshi.com/watch/1500564.html.

[13] A section tunnel construction organization design getting the Luban Prize for Construction Project via single-hole double-line slurry pressurized balanced shield, https://jz.docin.com/p-1949811535.html?building=1&fid=1472, (2015).

[14] X. Zhao, N. Singhaputtangkul, Effects of firm characteristics on enterprise risk manage-ment: case study of Chinese construction firms operating in Singapore, J. Manag. Eng. 32 (4) (2016) 05016008https://doi.org/10.1061/(ASCE)ME.1943-5479.0000434.

[15] B.G. Hwang, X. Zhao, G.S. Yu, Risk identification and allocation in underground rail construction joint ventures: contractors' perspective, J. Civ. Eng. Manag. 22 (6) (2016) 758–767, https://doi.org/10.3846/13923730.2014.914095.

[16] E. Perkins, Linking quality management and risk management, Quality Digest, 2011 https://www.qualitydigest.com/print/19354.

[17] L. Sarigiannidis, P.D. Chatzoglou, Quality vs risk: an investigation of their relationship in software development projects, Int. J. Proj. Manag. 32 (6) (2014) 1073–1082, https://doi.org/10.1016/j.ijproman.2013.11.001.

[18] M. Mikalsen, Quality and Risk Management in Projects (Master Thesis), Department of Production and Quality Engineering, Norwegian University of Science and Technology, 2012, https://core.ac.uk/download/pdf/30829393.pdf.

[19] M.A. Samani, N. Ismail, Z. Leman, N. Zulkifli, Quality management system and risk management system: similarities and possibilities for integration, Applied Mechanics & Materials. 564 (2014) 700–705, https://doi.org/10.4028/www.scientific.net/AMM.564.700.

[20] S. Zeng, J. Shi, G. Lou, A synergetic model for implementing an integrated management system: an empirical study in China, J. Clean. Prod. 15 (18) (2007) 1760–1767, https://doi.org/10.1016/j.jclepro.2006.03.007.

[21] K. Čekanová, Integrated management system – scope, possibilities and methodology, Research Papers Faculty of Materials Science and Technology in Trnava 23 (36) (2015) 135–140, https://doi.org/10.1515/rput-2015-0016.

[22] Y. Mao, T. Xu, Research of 4M1E's effect on engineering quality based on structural equation model, Systems Engineering Procedia. 1 (2011) 213–220, https://doi.org/10.1016/j.sepro.2011.08.034.

[23] C.U. Pyon, M.J. Lee, S.C. Park, Decision support system for service quality management using customer knowledge in public service organization, Expert Syst. Appl. 36 (4) (2009) 8227–8238, https://doi.org/10.1016/j.eswa.2008.10.021.

[24] B. Jeon, S.H. Suh, Design considerations and architecture for cooperative smart fact-ory: MAPE/BD approach, Procedia Manufacturing. 26 (2018) 1094–1106, https://doi.org/10.1016/j.promfg.2018.07.146.

[25] L. Zhang, X. Wu, L. Ding, M.J. Skibniewski, Y. Lu, Bim-based risk identification System in tunnel construction, Civil Engineering and Management. 22 (4) (2016) 529–539, https://doi.org/10.3846/13923730.2015.1023348.

[26] L. Zhang, X. Wu, L. Ding, Risk identification expert system for metro construction based on BIM, 2013 Proceedings of the 30th ISARC, Montréal, Canada, 2013, pp. 1437–1446, , https://doi.org/10.22260/ISARC2013/0163.

[27] H. Du, J. Du, S. Huang, GIS, GPS, and BIM-based risk control of Subway Station construction, ICTE 2015 (2015) 1478–1485 https://doi.org/10.1061/9780784479384.186.

[28] L. Ding, Y. Zhou, B. Akinci, Building information modeling (BIM) application framework: the process of expanding from 3D to computable nD, Autom. Constr. 46 (2014) 82–93, https://doi.org/10.1016/j.autcon.2014.04.009.

[29] J. Wang, W. Sun, W. Shou, X. Wang, C. Wu, H.Y. Chong, Y. Liu, C. Sun, Integrating BIM and LiDAR for real-time construction quality control, Journal of Intelligent & Robo-Tic Systems. 79 (3–4) (2015) 417–432, https://doi.org/10.1007/s10846-014-0116-8.

[30] J. Chen, J.H. Chen, Research in Establishment of Quality Control and Risk Managem-Ent Systems, 2011 Proceedings of the 28th ISARC, Seoul, Korea, (2011), https://doi.org/10.22260/ISARC2011/0057.

[31] R. Srinivasan, C. Kibert, S. Thakur, I. Ahmed, P. Fishwick, Z. Ezzell, J. Lakshmanan, Preliminary research in dynamic-BIM (D-BIM) workbench development, Winter Simulation Conference, IEEE Publications, 2012, pp. 1–12, https://doi.org/10.1109/WSC.2012.6465331.

[32] A.R. Pradhan, An Approach for Fusing Data From Multiple Sources To Support Constructi-on Productivity Analyses (Ph.D. Thesis), Department of Civil and Environment Engineering, University Carnegie Mellon, 2009, https://search.proquest.com/docview/304864742?accountid=15169.

[33] A. Pradhan, B. Akinci, C.T. Hass, Formalisms for query capture and data source identi-fication to support data fusion for construction productivity monitoring, Autom. Constr. 20 (4) (2011) 389–398, https://doi.org/10.1016/j.autcon.2010.11.009.

[34] S. Razavi N., C.T. Haas, Multisensor data fusion for on-site materials tracking in constr-uction, Autom. Constr. 19 (8) (2010) 1037–1046, https://doi.org/10.1016/j.autcon.2010.07.017.

[35] S.M. Shahandashti, S.N. Razavi, L. Soibelman, M. Berges, C.H. Caldas, I. Brilakis, J. Teizer, P.A. Vela, C. Haas, J. Garrett, B. Akinci, Z. Zhu, Data fusion approaches and applications for construction engineering, Journal of Construction Engineering & Management. 137 (10) (2011) 863–869, https://doi.org/10.1061/(ASCE)CO.1943-7862.0000287.

[36] L. Zhang, L. Ding, X. Wu, M.J. Skibniewski, An improved Dempster–Shafer approach to construction safety risk perception, Knowl.-Based Syst. 132 (2017) 30–46, https://doi.org/10.1016/j.knosys.2017.06.014.

[37] G. Shafer, A Mathematical Theory of Evidence, Princeton University Press, Princeton, 1976 (978-0691100425).

[38] J. Li, J.P. Wang, N. Xu, Z. Zhou, Analysis of safety risk factors for metro construction based on text mining method, tunnel, Construction. 37 (2) (2017) 160–166, https://doi.org/10.3973/j.issn.1672-741X.2017.02.006.

[39] Y. Zhu, Y.P. Li, G.H. Huang, L. Guo, Risk assessment of agricultural irrigation water under interval functions, Stoch. Env. Res. Risk A. 27 (2013) 693–704, https://doi.org/10.1007/s00477-012-0632-7.

[40] X. Wu, J. Duan, L. Zhang, S.M. AbouRizk, A hybrid information fusion approach to safety risk perception using sensor data under uncertainty, Stochastic Environmental Research and Risk. 32 (2018) 105–122, https://doi.org/10.1007/s00477-017-1389-9.
[41] Q. Cai, The design of software for analyzing of the dynamic physiological changes according to heart rate, Chinese Ergonomics. 6 (2) (2000) 20–23, https://doi.org/10.13837/j.issn.1006-8309.2000.02.006.
[42] W. Guo, X. Guo, X. Wan, Fatigue analysis system with HR and HRV as indexes, Chinese Medical Equipment Journal. 26 (8) (2005) 1–2, https://doi.org/10.3969/j.issn.1003-8868.2005.08.001.
[43] H. Guo, Y. Yu, T. Xiang, H. Li, D. Zhang, The availability of wearable-device-based physical data for the measurement of construction workers' psychological status on site: from the perspective of safety management, Autom. Constr. 82 (2017) 207–217, https://doi.org/10.1016/j.autcon.2017.06.001.
[44] W. Li, F. Yan, W. Meng, B. Liu, Evaluation of security risk in building construction project based on entropy weight and extension theory, Journal of Hebei University of Engineering (Natural Science Edition). 32 (2) (2015) 105–108, https://doi.org/10.3969/j.issn.1673-9469.2015.02.026.
[45] H. Lv, P. Wang, L. Feng, Y. Ji, Identification, appraisal and control of hazard installations in construction engineering, J. Civ. Eng. Manag. 23 (1) (2006) 43–45, https://doi.org/10.3969/j.issn.2095-0985.2006.01.011.
[46] C.H. Chang, Y. Lin, H.P. Tserng, Distilling and managing engineers' experience in construction projects using a pattern approach, Construction Management & Economics. 26 (3) (2008) 209–223, https://doi.org/10.1080/01446190701819061.
[47] H. Zhang, Cause analysis and countermeasure of leakage slurry in shield tail seal of hydric shield machine, Railway Standard Design (8) (2009) 76–78, https://doi.org/10.13238/j.issn.1004-2954.2009.08.029.
[48] H. Pei, Discussion on shield tunneling construction technology of full section water-rich sand and pebble bed, Highway (7) (2013) 283–285, https://doi.org/10.3969/j.issn.0451-0712.2013.07.064.
[49] P. Tu, X. Wang, Study on experiment of subsea tunnel grouting material, Journal of Railway Science and Engineering. 07 (6) (2010) 60–64, https://doi.org/10.19713/j.cnki.43-1423/u.2010.06.011.
[50] L.A. Zadeh, A simple view of the Dempster-Shafer theory of evidence and its implicat-ion for the rule of combination, Fuzzy Sets, Fuzzy Logic, and Fuzzy Systems (1986), https://doi.org/10.1142/9789814261302_0033.
[51] P. Xu, Y. Deng, X. Su, S. Mahadevan, A new method to determine basic probability assignment from training data, Knowl.-Based Syst. 46 (1) (2013) 69–80, https://doi.org/10.1016/j.knosys.2013.03.005.
[52] H. Shah, S. Hosder, T. Winter, Quantification of margins and mixed uncertainties using evidence theory and stochastic expansions, Reliability Engineering & System Safety. 138 (2015) 59–72, https://doi.org/10.1016/j.ress.2015.01.012.
[53] W. Cai, The extension set and incompatibility problem, Journal of Scientific Exploration. 1 (1983) 81–93 https://www.researchgate.net/publication/312577431_The_extension_set_and_incompatibility_problem.
[54] Y. Yin, L. Sun, C. Guo, A policy of conflict negotiation based on fuzzy matter element particle swarm optimization in distributed collaborative creative design, Comput. Aided Des. 40 (10 − 11) (2008) 1009–1014, https://doi.org/10.1016/j.cad.2008.08.003.
[55] Z. Sheng, S. Zhao, X. Qi, C. Wang, On-Line measurement of production plan track based on extension matter-element theory, Third International Symposium on Neural Networks, Chengdu, China, 2006, pp. 906–913 https://link.springer.com/content/pdf/10.1007%2F11760191.pdf.
[56] F. Qi, Q. Wu, Z. Li, A. Wang, Study on information fusion method of extenics-based D-S evidential theory, Third International Conference on Biomedical Engineering and Informatics, IEEE Publications, 2010, pp. 2975–2978, , https://doi.org/10.1109/BMEI.2010.5639337.
[57] J. Chen, F. Zhang, C. Yang, C. Zhang, L. Luo, Factor and trend analysis of total-loss marine casualty using a fuzzy matter element method, Disaster Risk Reduction. 24 (2017) 384–390, https://doi.org/10.1016/j.ijdrr.2017.07.001.
[58] L. Zhang, Y. Huang, X. Wang, M.J. Skibniewski, Risk-based estimate for operational safety in complex projects under uncertainty, Appl. Soft Comput. 54 (2017) 108–120, https://doi.org/10.1016/j.asoc.2017.01.020.
[59] C.K. Murphy, Combining belief functions when evidence conflicts, Decis. Support. Syst. 29 (1) (2000) 1–9, https://doi.org/10.1016/S0167-9236(99)00084-6.
[61] C. Zhou, L.Y. Ding, Safety barrier warning system for underground construction sites using internet-of-things technologies, Autom. Constr. 83 (2017) 372–389, https://doi.org/10.1016/j.autcon.2017.07.005.
[62] Z. Zhou, Y.M. Goh, Q. Li, Overview and analysis of safety management studies in the construction industry, Saf. Sci. 72 (2015) 337–350, https://doi.org/10.1016/j.ssci.2014.10.006.
[63] X. Zhao, P. Wu, X. Wang, Risk paths in BIM adoption: empirical study of China, Eng. Constr. Archit. Manag. 25 (9) (2018) 1170–1187, https://doi.org/10.1108/ECAM-08-2017-0169.
[66] Ministry of housing and urban-rural development of the People's Republic of China, Code for Risk Management of Underground Works in Urban Rail Transit, GB50652-2011 China Building Industry Press, 2011, pp. 50–60 https://www.doczhi.com/p-216447.html.